

High-repetition-rate optical parametric chirped-pulse amplifier producing 1- μ J, sub-100-fs pulses in the mid-infrared

C. Erny¹, C. Heese¹, M. Haag¹, L. Gallmann¹, U. Keller¹

¹Physics Department, ETH Zurich, 8093 Zurich, Switzerland

*Corresponding author: gallmann@phys.ethz.ch

Abstract: We present a high-repetition-rate, femtosecond optical parametric chirped pulse amplifier (OPCPA). Its seed signal is obtained by difference frequency generation from the two-branch output of a commercially available Er:fiber laser amplifier. The optical parametric amplifier is pumped by a commercially available diode-pumped solid-state laser. In a two-stage amplification setup we have achieved a gain of 100'000, resulting in $\sim 1 \mu$ J femtosecond mid-infrared pulses in the wavelength range between 3 and 4 μ m and an amplification bandwidth of >300 nm at a repetition rate of 100 kHz. The pulses have been compressed to 92 fs by a 4-prism compressor.

©2009 Optical Society of America

OCIS codes: (140.7090) Ultrafast lasers; (190.4970) Parametric oscillators and amplifiers; (140.3580) Lasers, solid-state; (140.4050) Mode-locked lasers.

References and links

1. T. Südmeyer, S. V. Marchese, S. Hashimoto, C. R. E. Baer, G. Gingras, B. Witzel, and U. Keller, "Femtosecond laser oscillators for high-field science," *Nature Photonics* **2**, 599-604 (2008).
2. U. Keller, "Ultrafast solid-state lasers," in *Landolt-Börnstein. Laser Physics and Applications. Subvolume B: Laser Systems. Part I*, G. Herziger, H. Weber, and R. Proprawe, eds. (Springer Verlag, Heidelberg, 2007), pp. 33-167.
3. J. Limpert, F. Röser, T. Schreiber, and A. Tünnermann, "High-Power Ultrafast Fiber Laser Systems," *IEEE J. Sel. Top. Quantum Electron.* **12**, 233-244 (2006).
4. J. Rothhardt, S. Hädrich, D. N. Schimpf, J. Limpert, and A. Tünnermann, "High repetition rate fiber amplifier pumped sub-20 fs optical parametric amplifier," *Opt. Express* **15**, 16729-16736 (2007).
5. A. Steinmann, A. Killi, G. Palmer, T. Binhammer, and U. Morgner, "Generation of few-cycle pulses directly from a MHz-NOPA," *Opt. Express* **14**, 10627-10630 (2006).
6. M. Marangoni, R. Osellame, R. Ramponi, G. Cerullo, A. Steinmann, and U. Morgner, "Near-infrared optical parametric amplifier at 1 MHz directly pumped by a femtosecond oscillator," *Opt. Lett.* **32**, 1489-1491 (2007).
7. U. Emmerichs, S. Woutersen, and H. J. Bakker, "Generation of intense femtosecond optical pulses near 3 μ m with a kilohertz repetition rate," *J. Opt. Soc. Am. B* **14**, 1480-1483 (1997).
8. D. Brida, C. Manzoni, G. Cirmi, M. Marangoni, S. D. Silvestri, and G. Cerullo, "Generation of broadband mid-infrared pulses from an optical parametric amplifier," *Opt. Express* **15**, 15035-15040 (2007).
9. T. Fujii, and T. Suzuki, "Generation of sub-two-cycle mid-infrared pulses by four-wave mixing through filamentation in air," *Opt. Lett.* **32**, 3330-3332 (2007).
10. H. R. Telle, G. Steinmeyer, A. E. Dunlop, J. Stenger, D. H. Sutter, and U. Keller, "Carrier-envelope offset phase control: A novel concept for absolute optical frequency measurement and ultrashort pulse generation," *Appl. Phys. B* **69**, 327-332 (1999).
11. A. Dubietis, G. Jonusauskas, and A. Piskarskas, "Powerful femtosecond pulse generation by chirped and stretched pulse parametric amplification in BBO crystal," *Opt. Communications* **88**, 437-440 (1992).
12. I. N. Ross, P. Matousek, G. H. C. New, and K. Osvay, "Analysis and optimization of optical parametric chirped pulse amplification," *J. Opt. Soc. Am. B* **19**, 2945-2956 (2002).
13. F. Adler, K. Moutzouris, A. Leitenstorfer, H. Schnatz, B. Lipphardt, G. Grosche, and F. Tauser, "Phase-locked two-branch erbium-doped fiber laser system for long-term precision measurements of optical frequencies," *Opt. Express* **12**, 5872-5880 (2004).

14. C. Emy, K. Moutzouris, J. Biegert, D. Kühlke, F. Adler, A. Leitenstorfer, and U. Keller, "Mid-infrared difference-frequency generation of ultrashort pulses tunable between 3.2 and 4.8 μm from a compact fiber source," *Opt. Lett.* **32**, 1138-1140 (2007).
15. A. Baltuska, T. Fuji, and T. Kobayashi, "Controlling the carrier-envelope phase of ultrashort light pulses with optical parametric amplifiers," *Phys. Rev. Lett.* **88**, 133901 (2002).
16. Y. Deng, F. Lu, and W. H. Knox, "Fiber-laser-based difference frequency generation scheme for carrier-envelope-offset phase stabilization applications," *Opt. Express* **13**, 4589 (2005).
17. C. P. Hauri, P. Schlup, G. Arisholm, J. Biegert, and U. Keller, "Phase-preserving chirped-pulse optical parametric amplification to 17.3 fs directly from a Ti:sapphire oscillator," *Opt. Lett.* **29**, 1369-1371 (2004).
18. F. Tauser, F. Adler, and A. Leitenstorfer, "Widely tunable sub-30-fs pulses from a compact erbium-doped-fiber source," *Opt. Lett.* **29**, 516-518 (2004).
19. M. J. W. Rodwell, D. M. Bloom, and K. J. Weingarten, "Subpicosecond laser timing stabilization," *IEEE J. Quantum Electron.* **25**, 817-827 (1989).
20. N. Ishii, C. Y. Teisset, T. Fuji, S. Kohler, K. Schmid, L. Veisz, A. Baltuska, and F. Krausz, "Seeding of an eleven femtosecond optical parametric chirped pulse amplifier and its Nd/sup 3+/ picosecond pump laser from a single broadband Ti:Sapphire oscillator," *IEEE J. Sel. Top. Quantum Electron.* **12**, 173-180 (2006).
21. C. Emy, L. Gallmann, and U. Keller, "High-Repetition-Rate Femtosecond Optical Parametric Chirped-Pulse Amplifier in the Mid-Infrared," submitted (2008).
22. B. Proctor, and F. Wise, "Quartz prism sequence for reduction of cubic phase in a modelocked Ti:sapphire laser," *Opt. Lett.* **17**, 1295-1297 (1992).
23. F. J. Duarte, "Generalized multiple-prism dispersion theory for pulse compression in ultrafast dye lasers," *Opt. Quantum Electron.* **19**, 223-229 (1987).
24. R. L. Fork, O. E. Martinez, and J. P. Gordon, "Negative dispersion using pairs of prisms," *Opt. Lett.* **9**, 150-152 (1984).
25. R. Trebino, and D. J. Kane, "Using phase retrieval to measure the intensity and phase of ultrashort pulses: frequency-resolved optical gating," *J. Opt. Soc. Am. A* **10**, 1101-1111 (1993).
26. M. Charbonneau-Lefort, B. Afeyan, and M. M. Fejer, "Optical parametric amplifiers using nonuniform quasi-phase-matched gratings. II. Space-time evolution of light pulses," *J. Opt. Soc. Am. B* **25**, 680-697 (2008).
27. M. Charbonneau-Lefort, B. Afeyan, and M. M. Fejer, "Optical parametric amplifiers using chirped quasi-phase-matching gratings I: practical design formulas," *J. Opt. Soc. Am. B* **25**, 463-480 (2008).

1. Introduction

Femtosecond mid-infrared laser sources are interesting for many applications ranging from vibrational spectroscopy for trace gas detection to strong-field laser-matter interactions. All of these applications benefit from high-repetition rate sources to reduce measurement time or to increase detection sensitivity [1]. With no suitable conventional gain materials in the mid-infrared range, femtosecond pulses are typically generated through nonlinear frequency conversion. The rapid progress in SESAM mode-locked diode-pumped solid-state lasers [2] and high power ultrafast fiber laser systems [3] has enabled the push of optical parametric amplifiers (OPA) to repetition rates of hundreds of kHz to many MHz with moderately high pulse energies [4-6]. Such sources are efficient, relatively compact, simple, and affordable compared to more traditional OPA systems pumped by Ti:sapphire based technology but have been limited to the visible and near-infrared spectral region so far [4-6]. The generation of a high-average power 3.1-4.6 μm idler wave was mentioned in Ref. [6], but its output was not further characterized as the focus of this publication was on the signal wave located between 1.3 and 1.6 μm .

Most commonly, nonlinear frequency-conversion of femtosecond pulses into the mid-infrared around 3-4 μm employs intense pulses from Ti:sapphire amplifiers. Such systems routinely produce pulses with durations around 100 fs [7]. Recently, several sources delivering significantly shorter pulses through noncollinear optical parametric amplification (NOPA) [8] and four-wave mixing [9] at a mid-infrared output power of a few mW have been demonstrated.

Here, we present a novel approach for a femtosecond mid-infrared laser source delivering potentially carrier-envelope offset phase (CEP, [10]) stable pulses at high repetition rates. It is based on optical parametric chirped-pulse amplification (OPCPA) [11, 12] and uses a commercially available diode-pumped solid-state laser as its pump and a commercial fiber

laser amplifier for the CEP-stable seed generation. The pump laser is a Duetto from Time-Bandwidth-Products, whereas the mid-infrared seed signal is generated through difference frequency mixing of the two-branch-output from a Er: fiber laser amplifier (FFS from Toptica) [13, 14]. The difference frequency mixing signal is intrinsically CEP-stable [15, 16] and is expected to remain so even after amplification in an OPA pumped by an unstabilized laser [17]. Our OPCPA system produces sub-100-fs pulses with a pulse energy of up to $\sim 1 \mu\text{J}$ at a repetition rate of 100 kHz. To our knowledge this is the highest repetition rate from a mid-infrared OPCPA laser system. The generated pulses have an optical bandwidth of $>300 \text{ nm}$ and the central wavelength can be selected between $3.5 \mu\text{m}$ and $3.7 \mu\text{m}$.

2. OPCPA design and results

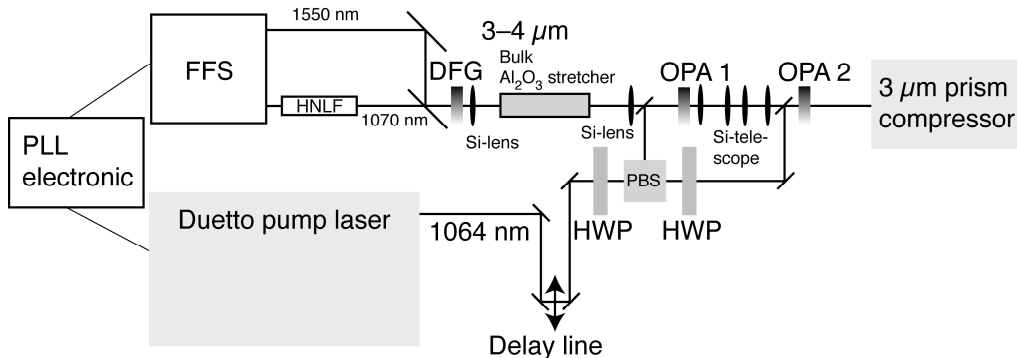


Fig. 1. Schematic setup of our OPCPA system. The three nonlinear optical stages DFG, OPA 1, and OPA 2 are based on MgO:PPLN crystals with lengths of 2 mm, 3 mm, and 1.4 mm, respectively. Lenses in the pump beam are not shown. (HWP, half-wave plate; PBS, polarizing beam splitter cube; HNLF, highly nonlinear fiber; FFS, fiber amplifier system).

A schematic setup of our OPCPA system is shown in Fig. 1. The system configuration takes the form of a two-stage amplifier optimized for broadband output between 3 and $4 \mu\text{m}$. The OPCPA seed is generated through difference frequency generation (DFG) from the two outputs of a commercially available two-branch Er: fiber laser/amplifier system and has been discussed in detail elsewhere [14]. In summary, one output of the $1.5 \mu\text{m}$ fiber laser is spectrally shifted in a highly nonlinear fiber to 1070 nm [18] and collinearly overlapped with the beam from the other branch in a 2 mm long MgO:PPLN crystal. In this DFG stage, up to 1 mW of mid-infrared radiation is generated at the full 82 MHz repetition rate of the fiber laser. This corresponds to a pulse energy of 12 pJ. The full-width-at-half-maximum (FWHM) spectral bandwidth reaches up to 360 nm. Using a MgO:PPLN device with a fan-out design permits us to tune the generated mid-infrared radiation between 3.4 and $4.8 \mu\text{m}$. Simulations show that the pulses can be assumed to be close to their transform limit with a duration between 55 fs and 60 fs. This corresponds to about 5 optical cycles at $3.5 \mu\text{m}$.

The Duetto pump laser in Fig. 1 is a Nd:YVO₄ based amplifier system operating at 1064 nm. Its repetition rate is tunable between 30 and 100 kHz and it provides 10 ps pulses with a pulse energy of $100 \mu\text{J}$ at 100 kHz. Due to unoptimized beam routing and lossy optics, only $55 \mu\text{J}$ of total pump energy are used in our experiments. The pulse trains from the seed and the pump laser are locked to each other electronically with a commercial phase locked loop (PLL) detector (CLX-1100 from Time-Bandwidth-Products) [19]. We have employed the fiber laser as the master oscillator and are controlling the output of the oscillator of the Duetto. The residual in-loop timing jitter amounts to 170 fs rms. Although direct optical stabilization schemes could potentially provide better stability [20], these are difficult to implement for our system. Simulations show that the measured timing jitter is sufficiently low for our OPCPA design.

The mid-infrared seed signal is first collimated by an anti-reflection (AR) coated Si-lens with 30 mm focal length. The seed is then separated from the other two waves at $1.1 \mu\text{m}$ and

1.6 μm that are also present in the DFG stage by passing the beam through a germanium wafer under Brewster's angle. The seed pulses are temporally stretched in 50 mm of bulk sapphire (Al_2O_3) providing total group delay dispersion (GDD) of about $-50'000 \text{ fs}^2$ and third order dispersion (TOD) of $330'000 \text{ fs}^3$ at 3.5 μm . This stretches the input pulse to a duration of 2.4 ps. While one would expect to achieve the best conversion efficiency with a seed pulse duration approximately matching to the pump pulse duration, we optimized our system for maximum amplification bandwidth. Simulations reveal that the highest amplification bandwidth for our OPCPA design can be achieved with a signal pulse duration in the range of 1 to 3 ps. Furthermore, simulations also show that we obtain larger output bandwidth by operating the first OPA in strong gain saturation. In this regime, the pump pulse is saturated first around the peak of the seed pulse. The temporal wings of the strongly linearly chirped input pulse saturate their gain later and may thus experience a larger overall amplification factor for a sufficiently long nonlinear medium. This leads to a spectral broadening due to the frequency-to-time mapping resulting from the strong chirp. A seed pulse that is too long, on the other hand, experiences time-dependent gain leading to gain narrowing. A more detailed discussion of these effects and our simulations is given in Ref. [21].

The stretched 3.5 μm seed signal with 0.8 mW of average power and 9.8 pJ pulse energy is refocused by a Si-lens with 75 mm focal length into the first OPA stage. The resulting $1/e^2$ beam radius is 42 μm . The measured seed spectrum is shown in the left-most part of Fig. 2. The first OPA consists of a 3 mm long, uncoated MgO:PPLN crystal with 7 different quasi-phase matching (QPM) grating periods (28.76, 29.30, 29.86, 30.46, 31.10, and 31.78 μm). The selected gratings allow phase-matching a 1.064 μm pumped OPA between 2.5 μm and 4.0 μm . This covers the main operation range of our DFG seed source. For our experiments, we fully characterized the system with phase-matched center wavelengths of 3.5 μm and 3.7 μm . The results at 3.7 μm are discussed at the end of this section.

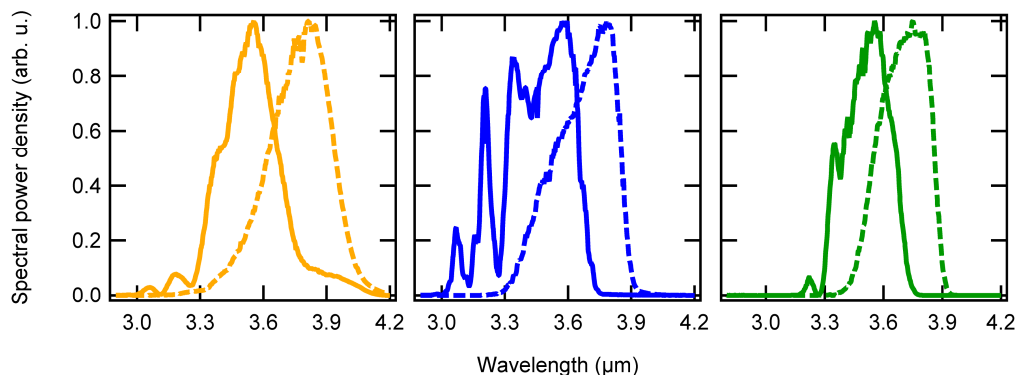


Fig. 2. Measured and normalized mid-infrared spectra directly after the DFG seed source (left), after the first amplification stage (middle) and after the second amplification stage (right). All spectra were recorded with a scanning monochromator equipped with a HgCdTe (MCT) photodiode connected to a lock-in amplifier. The solid lines correspond to the OPCPA operating at a center wavelength of 3.5 μm , whereas the dashed lines show operation at 3.7 μm .

The time delay between the pump and seed pulses is fine-tuned with an optical delay line. A coarse tuning of the delay is achieved with the electrical signal cable length between the two PLL detector photodiodes near the two oscillators and the PLL electronics. After the delay line, the pump beam is split into a small part used to pump the first OPA (4.7 μJ) and the rest pumping the second OPA stage (47 μJ). The pump beam for the first OPA is focused by a lens with 250 mm focal length and overlapped collinearly with the seed beam on a dichroic mirror. The resulting pump beam radius reaches a $1/e^2$ value of 49 μm inside the PPLN. The effective pump energy is 3.9 μJ after accounting for the reflection losses on the uncoated nonlinear crystal. This is sufficient to amplify the seed signal to 9.7 mW average power or 97 nJ pulse energy at a central wavelength of 3.5 μm and the 100 kHz repetition rate of the

pump. The amplified signal is then separated from the idler wave located at $1.58\ \mu\text{m}$ and the pump at $1.064\ \mu\text{m}$ by transmission through a germanium wafer under Brewster's angle. The signal beam is subsequently recollimated by an AR coated Si-lens with 75 mm focal length. The measured FWHM bandwidth of the amplified spectrum after the first OPA stage is 340 nm (see Fig. 2, middle).

A telescope consisting of two Si lenses with 200 mm and -100 mm focal length then reduces the size of the output beam from the first OPA. This beam is refocused by another Si-lens with 150 mm focal length. The remaining pump beam passes through another optical delay line for fine tuning of the delay inside the second OPA and is then focused by a 250 mm focusing lens. Again, the pump and the signal beam are overlapped collinearly on a dichroic mirror. The measured focal beam radii amount to $180\ \mu\text{m}$ for both beams.

The second OPA stage consists of an uncoated, 1.4 mm long MgO:PPLN crystal. By pumping the second OPA with an effective $39\ \mu\text{J}$, the signal is amplified to $0.95\ \mu\text{J}$, corresponding to an average power of 95 mW. The measured spectral FWHM spans 332 nm at $3.5\ \mu\text{m}$, supporting 79 fs pulses (see Fig. 2, right). This corresponds to 6 to 7 optical cycles at this wavelength.

We have measured a parametric superfluorescence background of 0.4 mW after the first amplifier and 5 mW after the second amplification stage when blocking the seed beam. This may serve only as a worst-case estimate for the actual superfluorescence background.

The mid-infrared signal is separated from the pump by a dichroic mirror. This is to prevent an unnecessary thermal load in the collimating Si-lens through the unused pump light. Without this dichroic mirror, we observed damage to the mid-infrared AR coating of the lens and distortions of the transmitted beam. The idler beam is only partially removed by the dichroic mirror. A small fraction of the reflected idler is sent onto a photodiode and used as part of a slow feedback loop stabilizing the pump-seed delay. This ensures long-term stability even in the presence of room temperature and air pressure fluctuations. A lens with 100 mm focal length recollimates the final output beam after the second OPA.

When the OPCPA is operated at $3.7\ \mu\text{m}$ (dashed lines in Fig. 2), 0.5 mW of DFG seed power are amplified to 9.6 mW in the first OPA. The output power after the second OPA amounts to 88 mW. The bandwidth was measured to 326 nm FWHM after the DFG, which is subsequently broadened to 331 nm in the first OPA. The output bandwidth after the second amplification stage was 313 nm and supports 87 fs pulses.

3. Pulse compression and characterization

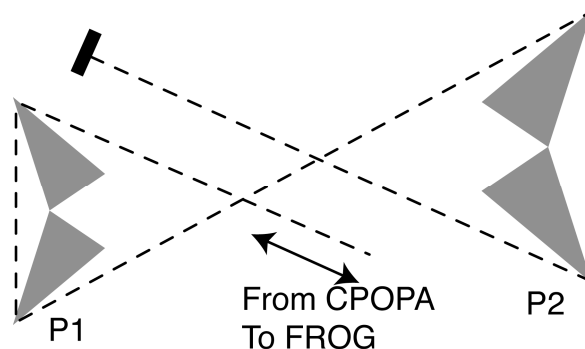


Fig. 3. 4-prism compressor setup based on two pairs of silicon prisms (P1 and P2).

We have compressed the output of the OPCPA system with a 4-prism compressor, where the beam passes the four uncoated silicon prisms under Brewster's angle (Fig. 3, [22, 23]). Simpler compressors such as bulk silicon, which provides the opposite sign of GDD compared to sapphire and LiNbO₃, or a classical two-prism compressor [24] can also introduce the desired amount of GDD. However, these simpler approaches possess the same sign of third order dispersion (TOD) compared to sapphire and LiNbO₃. In contrast to the 4-

prism compressor, they are therefore not suitable for TOD compensation. The relatively high refractive index of silicon yields a Brewster's angle of 73.7° . This results in the beam geometry shown in Fig. 3, where the total beam deflection angle over one prism pair is larger than 180° . As a consequence, the different beams cross in the middle of the two prism pairs depending on the required prism apex distance. The amount of prism bulk material along the beam path can be increased by moving the two prism pairs towards the center of the compressor, unlike the behavior of more conventional prism compressors. So far, the throughput of our prism sequence was limited to 41%. This corresponds to a transmission of $\sim 90\%$ per prism. The main contribution to the losses is likely due to the non-optimum optical and material quality of our prisms.

With this setup we were able to compress the pulses to 92 fs. Pulse characterization was performed with second-harmonic generation frequency-resolved optical gating (SHG FROG, [25]). Our SHG FROG setup employed a $250\ \mu\text{m}$ thick silver gallium selenide (AgGaSe_2) crystal to generate the second harmonic signal. The generated spectra ranging from $1.5\ \mu\text{m}$ to $2\ \mu\text{m}$ have been measured with a scanning monochromator equipped with an extended InGaAs photodiode connected to a lock-in amplifier. The FROG trace was recorded on a (128×128) grid. The acquisition of a complete FROG trace in Fig. 4 took more than one hour because we had to scan both the monochromator grating and the pulse delay in the FROG setup. Thus, this measurement also serves as a demonstration of the stability of our OPCPA system.

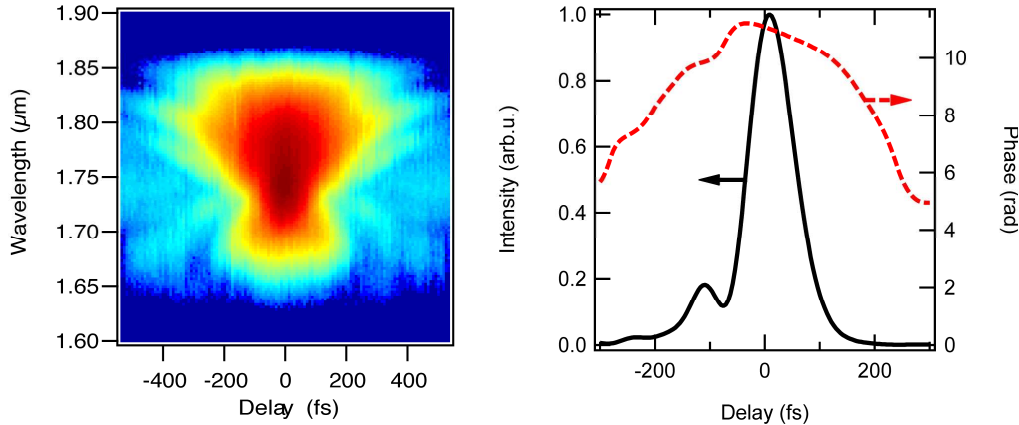


Fig. 4. Measured FROG trace (left) with retrieved pulse shape and phase (right)

4. Conclusion

We have demonstrated a femtosecond mid-infrared OPCPA laser system based on reliable, compact and commercially available solid-state and fiber laser technology. Our system operates at a high repetition rate of 100 kHz and delivers output pulses at center wavelengths of $3.5\ \mu\text{m}$ and $3.7\ \mu\text{m}$ with a pulse energy of $\sim 1\ \mu\text{J}$. We have compressed the pulses to a duration of 92 fs. To our knowledge this is the highest repetition-rate OPCPA system in the mid-infrared demonstrated so far. Future work will be directed at extending the amplification bandwidth by using chirped quasi-phase-matched devices for the OPA stages [26, 27] and to experimentally prove the CEP-stability of the output pulses. A more powerful pump source will be used to further increase pulse energy to ultimately make such a source available for strong laser field experiments.

Acknowledgments

We would like to acknowledge financial support by the NCCR Quantum Photonics (NCCR QP), research instrument of the Swiss National Science Foundation (SNSF) and thank Time-Bandwidth Products AG for their support with the DUETTO pump laser and the loan of the synchronization electronics CLX-1100.